Reflection mode XAFS investigations of reactively sputtered thin films

Dirk Lützenkirchen-Hecht and Ronald Frahm

Institut für Materialwissenschaften und FB 8 – Physik, Bergische Universität Gesamthochschule Wuppertal, Gaußstr. 20, 42097 Wuppertal, Germany.
Email: dirklh@uni-wuppertal.de

Amorphous Ta-oxide and Sn-nitride thin films were prepared by reactive sputter deposition on smooth float glass substrates and investigated ex situ using reflection mode XAFS. The absorption coefficient μ and its fine structure were extracted from the measured reflection mode XAFS spectra with a method based on the Kramers-Kronig transform. Bond distances, coordination numbers and Debye-Waller factors were determined by a detailed XAFS data analysis and compared to those of reference compounds. In addition, changes of the atomic short range order of the sputter deposited Ta_2O_5-films induced by a thermal heat treatment in ambient air were examined as a function of the annealing temperature.

Keywords: Reflection mode XAFS, Ta-oxide, Sn-nitride, sputter deposition, thin films.

1. Introduction

Thin film formation by sputtering usually involves the bombardment of a target material with accelerated ions, the evaporation of target material and its deposition on a substrate. If a reactive species such as oxygen or methane is present in the gas phase, a chemical reaction with the evaporated target material can occur, leading to the deposition of a chemical compound. In the past, reactive sputter deposition processes were widely used for the preparation of oxides, carbides, nitrides, silicides or oxy-nitrides. The surface and volume microstructure of the deposited compounds depend strongly on details of the preparation procedure. For example, depending on the N_2-pressure, the substrate temperature and the rf-power, crystalline as well as amorphous Sn-nitride films with varying Sn and N contents were found after reactive radio-frequency magnetron sputtering (Maruyama & Morishita, 1995). In the present study, reactively sputtered amorphous Ta-oxide and Sn-nitride thin films were investigated using reflection mode XAFS. Both materials have potential applications in microelectronic devices, Ta-oxide e.g. for the use as capacitor material in dynamic random access memories (e.g. McKinley & Sandler, 1996) or as gate insulator in metal-oxide-semiconductor field effect transistors (e.g. Matsui *et al.*, 1990). Sn-nitrides are of special interest due to their promising semiconducting and electrochromic properties (see Inoue *et al.*, 1998).

2. Experimental details

While Ta-oxide films of different thickness t (20 nm≤t≤150 nm) were prepared by reactive sputtering from a Ta metal target in pure O_2 ($p \approx 1.2 \times 10^{-2}$ mbar), the Sn-nitride films were deposited in pure N_2 atmospheres ($p \approx 1.2 \times 10^{-2}$ mbar) using a tin metal target. The base pressure of the vacuum vessel was $\approx 10^{-6}$ mbar. Float glass plates were used as substrates. X-ray reflectivity and X-ray scattering experiments revealed that the mean surface roughness of these substrates is ≈5-6 Å while the correlation length amounts to ≈420-450 nm (Keil *et al.*, 2000). XPS analysis was performed in order to check the chemical composition of the thin films samples. The Ta-oxide films gave a Ta/O ratio of about (0.39±0.01)/1; indicating that stochiometric Ta_2O_5 was formed. While only minor surface contaminations of carbon species were found on reactively sputtered Ta-oxide films, appreciable amounts of oxygen and carbon (ca. 5-10 atomic %) were detected on Sn-nitride films. These films revealed an Sn/N ratio of (2.11±0.06)/1, in agreement with recently published values for the same system (Maruyama & Morishita, 1995). From the binding energy E_B of the N1s peak ($E_B \approx 397.5$ eV) it can be deduced that the detected nitrogen is mainly bound as nitride. X-ray diffraction revealed that the Sn-nitride and the Ta_2O_5 films layers are generally X-ray amorphous.

The X-ray absorption experiments presented here were performed at the bending magnet station RÖMO II (Frahm, 1989) and the X-ray undulator beamline BW1 (Frahm *et al.*, 1995) at the DORIS III storage ring at HASYLAB (Hamburg, Germany). Double-crystal monochromators with flat Si(111), Si(311) or Si(511) crystals were used. Reflectivity EXAFS data were collected at room temperature in the vicinity of the Sn K-edge (29200 eV) and the L_3-edge of Ta (9881 eV). Incident and reflected intensities were measured by means of argon and nitrogen filled ionization chambers. Metal foils of the respective elements were measured in transmission between the second and a third ionization chamber in order to calibrate the energy scale of the monochromator simultaneously with each sample. Reference spectra were obtained in transmission from the related metal foils and polycrystalline β-Ta_2O_5, SnO, SnO_2 and Sn_3N_4 powders.

For the reflection mode XAFS data analysis, a reduced reflectivity given by $\chi_R(E)=(R(E)-R_0(E))/R_0(E)$ was calculated, where $\Delta R(E)=R(E)-R_0(E)$ is the fine structure of the reflectivity and R_0 the structureless background, respectively. $\chi_R(E)$ can also be described as a superposition of $\Delta\beta(E)$ and $\Delta\delta(E)$, i.e. $\chi_R(E)=a\,\Delta\beta(E)+b\Delta\delta(E)$, where $\beta=\beta_0+\Delta\beta$ and $\delta=\delta_0+\Delta\delta$ are the imaginary and the real part of the complex refractive index, each containing oscillating ($\Delta\beta$, $\Delta\delta$) and non-oscillating (β_0, δ_0) contributions (Borthen & Strehblow, 1995). With β_0 and δ_0 from reflectivity versus glancing angle curves measured for several energies below and above the absorption edge of interest, the factors a and b can be determined by means of a Kramers-Kronig data transform of the reduced reflectivity fine structure and a simple least square fit of the results (Borthen & Strehblow, 1995). Thus, this procedure enables the extraction of the absorption coefficient $\mu=4\pi\beta/\lambda$ and its fine structure $\chi=\Delta\mu/\mu_0$ from the reflection mode XAFS data. This method has proven to give reliable results for several different sample systems in the past (e.g. Hecht *et al.*, 1997, Lützenkirchen-Hecht & Frahm, 2000).

3. Results and Discussion

In Fig. 1, reflection mode XAFS spectra obtained from a reactively sputtered Ta_2O_5 film (thickness $t \approx 22.4$ nm) are presented for several different glancing angles. Only weak XAFS oscillations could be detected. The absorption fine structure $\chi(k)*k^3$ extracted from the four individual reflectivity data sets are presented in the insert of Fig. 1; the high reproducibility is

obvious. Compared to the absorption fine structure data of polycrystalline β-Ta_2O_5, several small differences can be seen, most clearly between k=4 $Å^{-1}$ and 5.5 $Å^{-1}$.

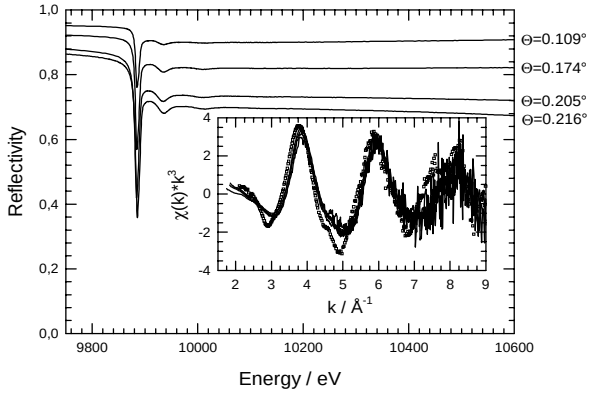

Figure 1:

Reflection mode XAFS scans from a reactively sputtered Ta_2O_5 film at the Ta L_3 edge for several glancing angles as indicated. Insert: Comparison of the absorption fine structure $\chi(k)*k^3$ extracted from the reflectivity data (——) and transmission XAFS data of a polycrystalline β-Ta_2O_5 reference sample ( ).

In Fig. 2, the magnitudes of the Fourier-Transforms for the thin film samples are compared to the reference compound. The intensity of the nearest Ta-O neighbor peak at around 1.5 Å radial distance is significantly smaller for the thin film samples. Although the thin films are X-ray amorphous as proven by X-ray diffraction, contributions of higher order shells are clearly visible at ≈2.7 Å and ≈3.3 Å. These are, however, more developed in the case of the β-Ta_2O_5 reference material, which reveals further contributions of higher coordinations at 4.2 and 5 Å radial distance, which are absent for the thin sputter deposited films. The data corresponding to first coordination (0.8 Å ≤ R ≤ 2.1 Å) were isolated as sketched in Fig. 2, backtransformed into k-space and fitted with a single Ta-O coordination shell. Phases and amplitudes were calculated using the FEFF code (Rehr *et al.*, 1992). The fit results are compiled in Tab. 1.

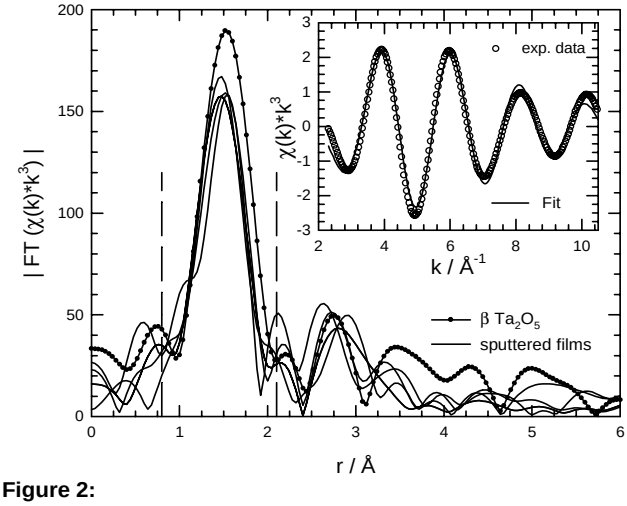

Figure 2:

Magnitudes of the Fourier-Transforms of the extracted fine structure data ($\chi(k)*k^3$) of Fig. 1 (— thin films samples, –●– β-Ta_2O_5). The data are not phase shift corrected. Insert: Fit of the back-transformed data corresponding to the first Ta-O coordination (0.8 Å ≤ R ≤ 2.1 Å, vertical dashed lines).

In general, the thin films reveal smaller bond distances compared to the bulk reference; this is a typical feature for amorphous samples (Cargill *et al.*, 1983, Frahm *et al.*, 1984). In addition, a significantly reduced coordination number N_1 and a slightly reduced σ_1 were determined for the thin film samples. This apparently reduced coordination number together with the smaller bond distance is a further indication for a highly disordered material and originates from the highly asymmetric pair distribution functions in amorphous solids: On the one hand, the repulsive part of the pair potential gives narrower distance distributions (i.e. smaller values for σ). On the other hand, EXAFS probes high values in momentum space and is therefore very sensitive to a broadening of the pair correlation functions (Cargill *et al.*, 1983, Frahm *et al.*, 1984). A detailed analysis of the cumulants – which can further clarify this situation – is currently under way.

Table 1:

Summary of the XAFS data analysis of the Ta_2O_5 samples: Bond distances R_1, coordination numbers N_1 and root mean square displacement σ_1 for the first Ta-O shell of reactively sputtered amorphous Ta_2O_5 thin films and polycrystalline β-Ta_2O_5. Crystallographic data are given for β-Ta_2O_5 for comparison (Airbrother, 1967).

	Ta_2O_5 thin films	Polycrystalline β-Ta_2O_5	Crystallographic Data
R_1 / Å	1.925 ± 0.020	1.971 ± 0.010	1.95 – 2.05
N_1	4.48 ± 0.09	6.04 ± 0.06	6
σ_1 / Å	0.097 ± 0.002	0.102 ± 0.001	---

Annealing of the Ta_2O_5 films was performed for temperatures between 100°C and 500°C in ambient air for two hours. X-ray diffraction proves that the films are still amorphous after this heat treatment. Only for the films annealed at 500°C, a small reduction of the amorphous background in the XRD-patterns was found. However, the analysis of the X-ray absorption data reveals several changes after the annealing procedure. This is illustrated in Fig. 3, where the Fourier-Transform of a thin film in the as deposited state is compared to that of an annealed film and to polycrystalline β-Ta_2O_5. The increase in intensity of the first coordination shell at ≈1.5 Å after annealing the Ta_2O_5 film at 500°C for two hours is obvious. However, the peak is still smaller compared to polycrystalline β-Ta_2O_5.

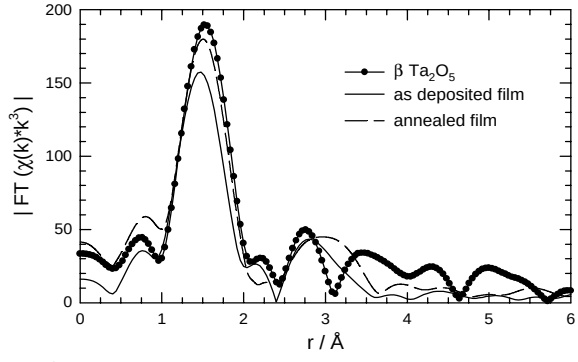

Figure 3:

Comparison of the magnitudes of the Fourier-Transforms of the extracted fine structure data $\chi(k)*k^3$ of a reactively sputtered Ta_2O_5 film in the as-deposited (——) and the annealed state (2h at 500°C, - - - -) and β-Ta_2O_5 (–●–). The data are not phase shift corrected.

More distinct changes were observed for the bond distances and coordination numbers derived from detailed evaluation of the

reflection mode XAFS spectra; these values are compiled in Tab. 2. Although the Ta-O bond distance increases from 1.925 Å to about 1.945 Å, it is still considerably smaller than that derived for β-Ta_2O_5. This observation is in qualitative agreement with the XRD experiments which suggests that the annealed films are in an amorphous state. The dramatic increase of N_1 found after the heat treatment as well as the slight increase of the bond distance might be indications of a rearrangement of the Ta and O atoms in the thin film. Annealing experiments at slightly higher temperatures or more extended annealing times are necessary to further clarify this interpretation.

Table 2:

Dependence of the structural parameters derived for the 1st Ta-O shell of reactively sputtered Ta_2O_5 thin films as a function of the annealing temperature.

Annealing temperature	R_1 / Å	N_1	σ_1 / Å
Room temperature	1.925 ± 0.020	4.48 ± 0.09	0.097 ± 0.002
400°C	1.946 ± 0.024	5.73 ± 0.06	0.101 ± 0.001
500°C	1.948 ± 0.050	5.25 ± 0.18	0.094 ± 0.003

In Fig. 4, reflectivity XAFS spectra obtained at the Sn K-edge from a reactively sputtered tin-nitride film (t≈120 nm) are presented. Only weak XAFS oscillations are visible. In the insert of Fig. 4, the normalized magnitude of the FT of the k^3-weighted reflectivity fine structures are presented for both spectra. Only a single, double peaked structure between ca 1.2 Å and 1.7 Å can be detected, in agreement with the absence of diffraction peaks in XRD experiments.

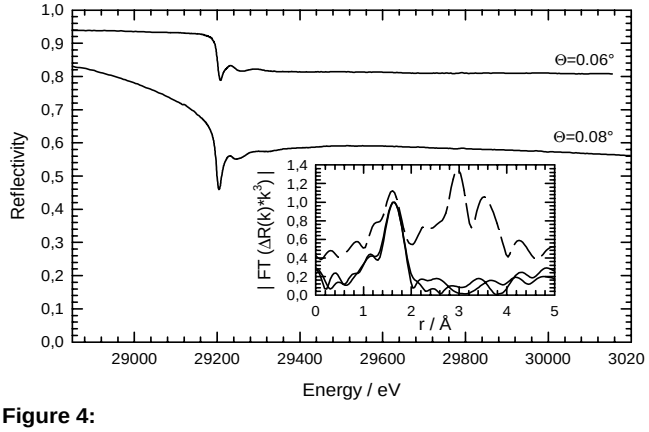

Figure 4:

Reflection mode XAFS spectra of a reactively sputtered Sn-N film (thickness ≈120 nm) at the Sn K-edge for two different glancing angles. The insert depicts normalized FT's of the k^3-weighted reflectivity fine structures $\Delta R(k)*k^3$ (full lines). For comparison, the normalized FT of polycrystalline Sn_3N_4 is also presented (dotted line, vertically shifted by 0.4). The data are not phase shift corrected.

The peak doublet between 1.2 Å and 1.7 Å corresponds well to the structures observed for polycrystalline Sn_3N_4, which crystallizes in a spinell structure ($MgAl_2O_4$-type, Scotti *et al.*, 1999). The two peaks can be associated with two different types of Sn ions which are present in this crystal structure: Sn(1) is coordinated by 4 N in a distance of 2.06 Å, and Sn(2) is in a octahedral symmetry with 6 N at about 2.17 Å radial distance (Lützenkirchen-Hecht *et al.*, 2000). Assuming Sn-N coordinations for both shells, a preliminary two shell model fit results in R_1≈1.97 Å and R_2≈2.2 Å for the first two peaks. Though these positions and the intensities of the individual shells correlate well to those observed for Sn_3N_4, the presence of two different Sn-N bonds with a similar atomic environment seems to be very likely. However, one should keep in mind that the XPS analysis indicated that the reactively sputtered Sn-nitride films are tin rich, while Sn_3N_4 is a nitrogen-enriched phase. In addition, oxygen is present in considerable amounts according to XPS studies, so that at least a fraction of the peak doublet might also be caused by Sn-O bonds. On the other hand, there is no similarity with a hexagonal structure as proposed by other goups (Lima *et al.*, 1991, Inoue *et al.*, 1998). Such a bond geometry would result in a single Sn-N bond distance of 2.46 Å, which is not at all consistent with our XAFS data. For the future, a more detailed XAFS data analysis and in-situ investigations of reactively sputtered Sn-nitride films are very desirable.

4. Conclusions

Reflection mode XAFS experiments were applied for the ex situ investigation of reactively sputtered thin films. The detailed data analysis suggests that the Ta-O bond distance is apparently smaller for amorphous Ta_2O_5 films compared to polycrystalline β-Ta_2O_5. After a thermal heat treatment in ambient atmosphere, a small increase of the Ta-O distance could be verified, although X-ray diffraction proves that the films are still amorphous. For amorphous Sn-nitride films, two different bond distances were found. The similarity of the determined bond lengths as well as the overall shape of the Fourier-Transform in this radial distance suggests a bond geometry similar to that in Sn_3N_4.

Acknowledgement

We like to thank S. Grundmann, H. Hammer, P. Keil and A. Krämer for their invaluable help during the measurements. Financial support by HASYLAB, the DFG and the MSWWF des Landes Nordrhein-Westfalen is is greatfully acknowledged.

References:

Airbrother, F. (1967). The chemistry of niobium and tantalum, Elsevier Publisher, Amsterdam, 30.
Borthen, P. & Strehblow, H.-H. (1995) *Phys. Rev.* **B 52**, 3017-3020.
Frahm, R., Haensel, R. & Rabe, P. (1984) *J. Phys. F: Met. Phys.* **14**, 1333-1342
Cargill, G.S., Weber, W. & Boehme, R.F. (1983), in EXAFS and Near Edge Structure, A. Bianconi, L. Incoccia and S. Stipcich (Eds.), Springer Verlag, Berlin (1983) 277 - 280.
Frahm, R. (1989). *Rev. Sci. Instr.* **60**, 2515 – 2518.
Frahm, R., Weigelt, J., Meyer, G. and Materlik, G. (1995). *Rev. Sci. Instrum.* **66**, 1677 – 1680.
Hecht, D., Borthen, P. & Strehblow, H.-H. (1997) *J. Phys. (France) IV* **C2**, 707 – 708
Inoue, Y., Nomiya, M. & Takai, O. (1998) *Vacuum* **51**, 673-676.
Keil, P., Lützenkirchen-Hecht, D. & Frahm, R. (2000) unpublished.
Lima, R.S., Dionisio, P.H., Schreiner, W.H. & Achete, C. (1991) *Sol. State Commun.* **79**, 395-398.
Lützenkirchen-Hecht, D. & Frahm, R. (2000) *Physica B* **283**, 108 –113.
Lützenkirchen-Hecht, D., Scotti, N., Jacobs, H. & Frahm, R. (2000). Submitted to J. Synchrotron Rad.
Maruyama, T. & Morishita, T. (1995) *J. Appl. Phys.* **77**, 6641-6645.
Matsui, M., Nagayoshi, H., Muto, G., Tanimoto, S., Kuroiwa, K. & Tarui, J. (1990) *Jpn. J. Appl. Phys.* **29**, 62-67.
McKinley, K.A. & Sandler, N.P. (1996). *Thin Sol. Films* **290/291**, 440-445.
Rehr, J.J., Albers, R.C. & Zabinsky, Z.I. (1992) *Phys. Rev. Lett.* **69**, 3397-3400.
Remy, J.C. & Hantzpergue, J.J. (1975) *Thin Sol. Films* **30**, 197-204.
Scotti, N., Kockelmann, W., Senker, J., Traßel, S. & Jacobs, H. (1999) *Z. Anorg. Allg. Chem.* **625**, 1435-1439.